

# RSC Advances



This is an *Accepted Manuscript*, which has been through the Royal Society of Chemistry peer review process and has been accepted for publication.

*Accepted Manuscripts* are published online shortly after acceptance, before technical editing, formatting and proof reading. Using this free service, authors can make their results available to the community, in citable form, before we publish the edited article. This *Accepted Manuscript* will be replaced by the edited, formatted and paginated article as soon as this is available.

You can find more information about *Accepted Manuscripts* in the [Information for Authors](#).

Please note that technical editing may introduce minor changes to the text and/or graphics, which may alter content. The journal's standard [Terms & Conditions](#) and the [Ethical guidelines](#) still apply. In no event shall the Royal Society of Chemistry be held responsible for any errors or omissions in this *Accepted Manuscript* or any consequences arising from the use of any information it contains.

# Computational Investigation of the Influence of tetrahedral oxoanions (sulphate, selenate and chromate) on the stability of Calcium Carbonate polymorphs

Cite this: DOI: 10.1039/x0xx00000x

Received 00th January 2012,  
Accepted 00th January 2012

DOI: 10.1039/x0xx00000x

[www.rsc.org/](http://www.rsc.org/)

M.E. Arroyo-de Dompablo<sup>1†</sup>, M.A. Fernández-González<sup>2</sup> and L. Fernández-Díaz<sup>3</sup>

The incorporation of tetrahedral  $\text{AO}_4^{2-}$  groups (A = S, Cr, Se) in  $\text{CaCO}_3$  polymorphs (calcite, aragonite and vaterite) is investigated from first principles calculations at the Density Functional Theory (DFT) level. We found that the less dense and softer vaterite crystal structure has the greater capability to distort accommodating tetrahedral ions. The calculated mixing enthalpies at 0 K of the  $\text{Ca}(\text{CO}_3)_{1-x}(\text{AO}_4)_x$  (A = S, Se, Cr) vaterite and calcite polymorphs are below 3 kJ/mol when  $x < 0.05$ , confirming that the incorporation of small concentration of tetrahedral groups is thermodynamically feasible in those polymorphs at moderate temperatures. Calcite is identified as the most stable polymorph at any investigated dopant concentration ( $0 < x < 0.25$ ). Although our results do not predict stability crossovers resulting from  $\text{AO}_4^{2-}$  groups incorporation into  $\text{CaCO}_3$  polymorphs, they strongly support a reduction of the driving force for the transformation of  $\text{AO}_4$ -bearing vaterite into the thermodynamically stable calcite.

## Introduction

Calcium carbonate is ubiquitous in nature, where it can have inorganic or biogenic origin.<sup>1</sup> Under Earth's surface conditions calcium carbonate can precipitate as three different crystalline anhydrous forms (vaterite, aragonite and calcite) and two hydrated forms (monohydrocalcite and ikaite).<sup>2</sup> Moreover, a variety of amorphous calcium carbonates (ACC) with different water contents and different degrees of order have been found in recent years as playing a major role in biomineralization processes.<sup>3</sup> Calcium carbonate also has important technological applications.<sup>4</sup> Undesired scaling resulting from calcium carbonate precipitation is a major problem in numerous industrial processes and households all over the world.<sup>5</sup>

Sulfate ( $\text{SO}_4^{2-}$ ), chromate ( $\text{CrO}_4^{2-}$ ) and selenate ( $\text{SeO}_4^{2-}$ ) are tetrahedral oxoanions of similar size. Sulfate is an abundant ion in both ground waters and seawater and a main component of sedimentary rocks.<sup>6</sup> Although chromate and selenate are far less abundant than sulfate, the concentration of both oxoanions in natural environments has been growing during the last century due to mining activities and the extended use of Cr and Se compounds in a variety of industries.<sup>7,8</sup> Chromate is a powerful mutagen and carcinogen.<sup>9</sup> Contrarily, selenate is considered not

to be toxic for organisms. However, the high radiotoxicity of the long-lived isotope  $^{79}\text{Se}$  has raised general concern on the spread of selenium compounds in natural waters and soils.<sup>10-12</sup> The incorporation of inorganic pollutants into the structure of stable sparingly soluble mineral phases, like e.g. calcite, is considered an effective means to long-term reduce the mobility and bioavailability of contaminants.<sup>13-15</sup>

Reeder and coworkers studied the incorporation of  $\text{SO}_4^{2-}$ ,  $\text{SeO}_4^{2-}$  and  $\text{CrO}_4^{2-}$  into synthetic calcite using synchrotron radiation based techniques and concluded that all three tetrahedral oxoanions substitute in the position occupied by  $\text{CO}_3^{2-}$  groups with significant disruption of the local structure<sup>16-18</sup>. It is well known that sulfate incorporates into natural calcite and aragonite of inorganic origin in concentrations that in calcite are 1.8 to 4.2 times those found in aragonite<sup>19</sup>. Biogenic calcium carbonates also contain significant sulfate concentrations (from several hundred to several thousand ppm<sup>20</sup>). Although this sulphur is commonly related to occluded organic matter<sup>21</sup>, a recent  $\mu\text{-XRF}$  ( $\mu\text{-XRF}$ ) and X-ray absorption near-edge structure (XANES) study of the local environment of sulfur in bivalve shells has demonstrated the presence of inorganic sulfate in both calcitic and aragonitic shells.<sup>22</sup>

Recent studies have shown that the crystallization of  $\text{CaCO}_3$  is strongly influenced by the presence of tetrahedral oxoanions in the growth medium. This influence translates into the stabilization of metastable phases in all the cases. Thus, different authors have reported that in the presence of chromate and selenate the formation of vaterite is promoted and the transformation of this phase into the stable calcite becomes progressively delayed as the concentration of these oxyanions in the growth medium is higher.<sup>23-25</sup> The influence of sulfate on  $\text{CaCO}_3$  crystallization seems to be far more complex: whereas different authors have concluded that the presence of sulfate induces a switch from calcite to aragonite<sup>26-29</sup>, other authors point to vaterite<sup>30-33</sup> becoming the predominant polymorph in sulfate-rich environments.

The possibility that the incorporation of certain ions induces changes in the relative stability of polymorphs is most relevant in the context of biomineralization studies, where understanding the factors that control  $\text{CaCO}_3$  polymorph selection has become a major issue<sup>34</sup>. Stability crossovers also need to be considered when designing strategies for the storage of contaminant elements in the structure of sparingly soluble minerals since the development of transformations between polymorphs could lead to the release of those pollutants to the environment. The growing concern over climate change is also promoting the exploration of methods for the long-term carbon dioxide sequestration. Some of these methods involve the introduction of supercritical carbon dioxide into deep aquifers.<sup>35</sup> The interaction between  $\text{CO}_2$ , the aqueous phase and the rock-stock will lead to the precipitation of  $\text{CaCO}_3$  through both, the reaction with dissolved calcium and the carbonation of rock-forming minerals.<sup>33, 36</sup> Since dissolved sulfate is ubiquitous in ground waters and calcium sulfate minerals like gypsum ( $\text{CaSO}_4 \cdot 2\text{H}_2\text{O}$ ) and anhydrite ( $\text{CaSO}_4$ ) are major constituents of evaporitic rocks, it is important in this context to understand the influence of sulfate oxoanions in the energetics of the  $\text{CaCO}_3$  system.

In this work we attempt to rationalize the factors that account for the observed  $\text{CaCO}_3$  polymorph selection in the presence of sulfate, chromate and selenate oxoanions. With this aim we have used computational methods to investigate the thermodynamic feasibility of incorporating the above mentioned tetrahedral groups in the  $\text{CaCO}_3$  polymorphs. In a previous work<sup>32</sup> we studied the incorporation of sulfate groups in  $\text{CaCO}_3$  polymorphs by atomistic model simulations. This computational technique requires empirical or semiempirical interatomic potentials, which are implemented in force fields. Good quality and transferable force fields are known for sulfates<sup>37</sup>, chromates<sup>38</sup> and carbonates<sup>39</sup>. However, to the best of our knowledge, reliable force fields have not been developed for selenates. Quantum-chemical calculations do not require any experimental input beyond the crystal structure and the nature of the constituent elements. This makes Density Functional Theory (DFT) a powerful tool to investigate the energetics of different compositions of the anionic solid solutions  $\text{Ca}(\text{CO}_3)_{1-x}(\text{AO}_4)_x$  (A= S, Se, Cr) considering different structural types (calcite, aragonite and vaterite).

**Crystal Structures.**—Calcite (S.G.  $R\bar{3}c$ ) is the most stable form of  $\text{CaCO}_3$  at ambient P and T conditions. Its crystal structure consists on carbonate groups perpendicular to the  $c$  axis with Ca atoms in octahedral coordination (**figure 1a**). Calcite transforms to the denser aragonite (S.G.  $Pmcn$ , **figure 1b**) at the upper mantle conditions. In such transformation the coordination of Ca ion increases to ninefold while the carbonate groups remain perpendicular to the  $c$  axis. Vaterite is a metastable  $\text{CaCO}_3$  polymorph at any P-T. The crystal structure of vaterite is still under debate. It is accepted that Ca ions are in eightfold coordination and carbonate groups lie parallel to the  $c$  axis. At room temperature vaterite is a dynamic structure; the rotation of the carbonate groups in the three possible orientations parallel to the  $c$  axis results in a disordered structure. Layer stacking and chirality introduce additional structural complexity.<sup>40, 41</sup> Along the years several crystal models has been postulated with tetragonal ( $Pbnm$ <sup>42</sup>,  $Ama2$ <sup>43</sup>), hexagonal ( $P6_3/mmc$ <sup>44</sup>,  $P6_522$ <sup>45</sup>,  $P3_221$ <sup>46</sup>,  $P6_322$ <sup>47</sup>) and monoclinic ( $C2/c$ <sup>41</sup>,  $C\bar{1}$ <sup>48</sup>) symmetries. Recent computational<sup>40, 46</sup> and experimental<sup>48</sup> investigations point to the coexistence in vaterite of various crystal structures exhibiting minor structural and energetic differences. **Figure 1c** shows the crystal structures of the  $Ama2$  and  $P6_3/mmc$  models, which together with the  $P6_522$  were computed in this work. The  $P6_522$  is an ordered superstructure of the  $P6_3/mmc$  disordered pseudo-cell.

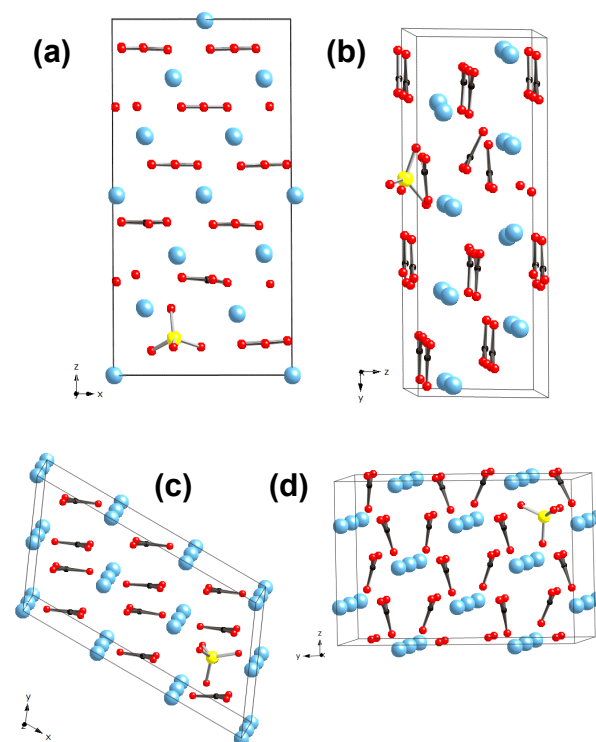


Fig. 1. Unit cell of the  $\text{Ca}(\text{CO}_3)_{1-x}(\text{AO}_4)_x$  crystal structures utilized in the calculations showing the incorporation of the tetrahedral  $\text{AO}_4$  groups (A = S, Se, Cr) to replace a triangular  $\text{CO}_3^{2-}$  polyanion. (a) calcite with  $x=0.056$ , (b) aragonite with  $x=0.063$  (c)  $P6_3/mmc$  vaterite with  $x=0.063$  and (d)  $Ama2$  vaterite with  $x=0.056$ . Color code: oxygen in red, carbon in black and A in yellow.

## Methodology

Total energy calculations based on Density Functional Theory (DFT) have been performed using the VASP package (Vienna ab-initio simulation program).<sup>49, 50</sup> within the General Gradient Approximation (GGA), with the exchange and correlation functional form developed by Perdew, Burke, and Ernzerhof (PBE).<sup>51</sup> Just valence electrons at C, O, S, and Se atoms are taken into account. For higher accuracy, the semi-core Cr (3p, 4s) and Ca (3s, 3p) states were treated as valence states. The introduction of the semi-core *p* states in the pseudopotential might be critical for early transition metals (V, Ti, Cr) (see for instance<sup>52, 53</sup>). The interaction of core electrons with the nuclei is described by the Projector Augmented Wave (PAW) method<sup>54</sup>. The energy cut off for the plane wave basis set was kept fix at a constant value of 600 eV throughout the calculations. Non-spin polarized calculations were performed in all cases. The integration in the Brillouin zone is done on an appropriate set of *k*-points determined by the Monkhorst-Pack scheme (for details see S.I.). All the structures were fully relaxed (atomic positions, cell parameters and volume). The default convergence criteria were used for both ionic and electronic loops. This led to a difference of the order of 10<sup>-3</sup> Å in lattice parameters and 10<sup>-2</sup> kJ/mol in the total energy. The final energies of the optimized geometries were recalculated so as to correct the changes in the basis set of wave functions during relaxation. All the parameters in the calculation were tested to provide a level of convergence of the total energy within 0.5 kJ/mol.

The initial cell parameters and atomic positions of calcite and aragonite were taken from Graf<sup>55</sup> and de Villiers<sup>56</sup>, respectively. For the structure of vaterite three different models were investigated; *P6<sub>5</sub>22* from Wang<sup>45</sup>, *Ama2* from Le Bail<sup>43</sup> and *P6<sub>3</sub>/mmc* from Kamhi<sup>44</sup>. From the original unit cells of calcite, aragonite and vaterite by Le Bail and by Kamhi, the supercells were built by adding complete cells in different directions a, b or/and c. In each supercell one of the CO<sub>3</sub><sup>2-</sup> groups was substituted by one AO<sub>4</sub><sup>2-</sup> group. The A atom of the AO<sub>4</sub><sup>2-</sup> tetrahedron was set to the position of the C atom of the CO<sub>3</sub> triangle in the original supercell. In the built supercells all the CO<sub>3</sub><sup>2-</sup> groups are symmetrically equivalent and therefore, any of them could have been substituted by AO<sub>4</sub><sup>2-</sup> with identical results. Moreover, for each explored substitution, at least 10 initial random orientations of the AO<sub>4</sub><sup>2-</sup> tetrahedron were tested, but they all converged to the same final orientation at the first stages of relaxation. More details about the supercells construction can be found in our previous work<sup>32</sup>. The number of CaCO<sub>3</sub> formula ranged from 4 to 48. Since in each supercell one of the CO<sub>3</sub><sup>2-</sup> groups was substituted by an AO<sub>4</sub><sup>2-</sup> group (A = S, Cr, Se), the doped structures can be formulated as Ca(CO<sub>3</sub>)<sub>1-x</sub>(AO<sub>4</sub>)<sub>x</sub> with 0.021 < x < 0.25. **Figure 1** shows selected examples of the computed structures. Estimation of mixing enthalpies i.e., the enthalpy difference between the doped Ca(CO<sub>3</sub>)<sub>1-x</sub>(AO<sub>4</sub>)<sub>x</sub> and the pure compounds CaCO<sub>3</sub> and CaAO<sub>4</sub> with A = S, Cr, Se, required calculating the total energy of anhydrite-CaSO<sub>4</sub><sup>57</sup>, chromatite-CaCrO<sub>4</sub><sup>58</sup> and CaSeO<sub>4</sub>. For the

latter, since no known mineral has the composition CaSeO<sub>4</sub>, the crystal structure of chromatite was also adopted.

Relaxed structure calculations were performed at various constant volumes and the energy-volume data was fitted to the Murnaghan equation of state<sup>59</sup>

$$E(V) = B_0 V_0 \left[ \frac{1}{B'(B'-1)} \left( \frac{V_0}{V} \right)^{B'-1} + \frac{V}{B'V_0} - \frac{1}{(B'-1)} \right] + E_0 \quad (1)$$

where  $B_0$  is the bulk modulus at zero pressure,  $B'$  its first derivative,  $E_0$  the minimum energy and  $V_0$  the volume at the minimum of energy.

## Results

**Table I** compares the calculated lattice parameters and bulk modulus for the fully relaxed structures of calcite, aragonite and *P6<sub>5</sub>22*-vaterite with the experimental ones. The calculated enthalpies vs. pressure (see S.I.) yield calcite as the stable phase at ambient pressure, while aragonite is predicted as the thermodynamically stable phase above 4 GPa in excellent agreement with the experimental transition pressure of 4GPa<sup>60</sup>. We can conclude that the used methodology correctly reproduce the lattice parameters, the transition pressure and the bulk modulus of CaCO<sub>3</sub> polymorphs.

TABLE I - Calculated lattice parameters, cell volume and bulk modulus and for CaCO<sub>3</sub> polymorphs calcite, aragonite and vaterite.

CaCO <sub>3</sub> Polymorph	Calculated a,b,c (Å) V (Å <sup>3</sup> )	Exp. a,b,c (Å) V (Å <sup>3</sup> )	Cal. B (GPa)	Exp. B (GPa)
Calcite	5.048, 5.048, 17.249 380.69	4.9900, 4.9900, 17.0615 367.916 <sup>55</sup>	71.4	73 <sup>61</sup>
Aragonite	5.009, 8.030, 5.796 233.16	4.9614, 7.9671, 5.7404 226.85 <sup>56</sup>	67.0	67.1 <sup>62</sup>
Vaterite <i>P6<sub>5</sub>22</i>	7.280, 7.280, 25.538 1172.29	-	60.4	-
(pseudocell)	4.203, 4.203, 8.513 130.23	4.13, 4.13, 8.49 <sup>44</sup> 125.41		

We have also calculated the total energy of other vaterite models, *Ama2*<sup>43</sup> and *P6<sub>3</sub>/mmc*<sup>44</sup>. **Figure 2** confronts our results with others reported in the literature<sup>41, 45, 46, 63-65</sup>, taking that of vaterite-*P6<sub>5</sub>22* as the zero of energy. Our calculated energy differences among vaterite-*P6<sub>5</sub>22*, calcite and aragonite agree with those reported by other authors using a similar set for the calculations. Regarding the vaterite structures, the most stable models are the hexagonal *P6<sub>5</sub>22* and *P3<sub>2</sub>11*, whose calculated total energies differ by less than 1.5 kJ/mol. The second hexagonal model that we tested, the disordered pseudocell of S.G. *P6<sub>3</sub>/mmc*, is 5.9 kJ/mol less stable than its ordered superstructure *P6<sub>5</sub>22*. In good agreement with other authors, we found the orthorhombic *Ama2* model quite unstable, with a



calculated total energy of 16.5 kJ/mol higher than that of the  $P6_322$  model.

From **figure 2** it is evident that important energy differences exist among the distinct vaterite models. Given the complexity of describing the vaterite with a unique crystallographic model it seems important to evaluate the effect of the crystal structure on the energetics of the incorporation of tetrahedral groups. In order to establish a comparison with our previous atomistic simulation investigation<sup>32</sup>, we have chosen the hexagonal  $P6_3/mmc$  model (10 atoms), which is a pseudo cell of the  $P6_322$  vaterite structure<sup>41</sup>. Supercell calculations for the most stable ordered models would be computationally very demanding (the unit cell of  $P6_322$  has 90 atoms). Hence we have also considered the orthorhombic vaterite *Ama2* (20 atoms) which, in spite of being one of the less stable models (see **figure 3**), is computationally affordable.

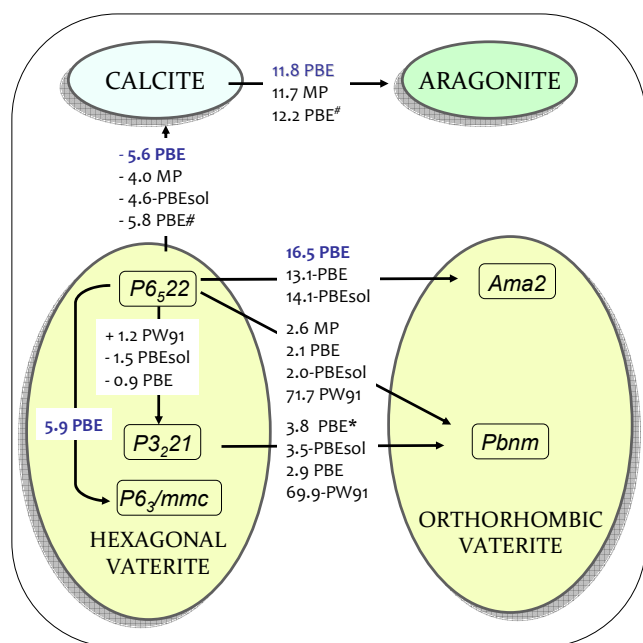
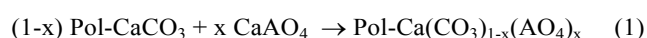


Figure 2.- Summary of calculated relative energetic stability of CaCO<sub>3</sub> polymorphs utilizing DFT methods (in kJ/mol). Models considered for the vaterite polymorphs are split in two groups: hexagonal models ( $P6_322$ ,  $P3_221$ ,  $P6_3/mmc$ ) and orthorhombic (*Ama2* and *Pbnm*). The zero of energy is set at the calculated energy for the vaterite- $P6_322$ . Reported data are taken from<sup>63</sup>(MP),<sup>46</sup>(PBE and PBE-sol),<sup>64</sup>(PBE\*),<sup>41</sup>(PBE#) and<sup>45</sup>(PW91). Energies calculated in this work are given in bold blue numbers.

**Mixing enthalpies.** The tendency of CaCO<sub>3</sub> polymorphs to incorporate tetragonal groups (substituting for a carbonate group) can be estimated from the enthalpy of mixing. This can be described as the enthalpy difference between the substituted Ca(CO<sub>3</sub>)<sub>1-x</sub>(AO<sub>4</sub>)<sub>x</sub> (A = S, Se, Cr) and the pure compounds CaCO<sub>3</sub> and CaAO<sub>4</sub>, according with the reaction:



Positive enthalpies of mixing represent a tendency for phase separation into the respective CaCO<sub>3</sub> polymorph (calcite, aragonite and vaterite) and CaAO<sub>4</sub> (anhydrite structure for A = S, and chromatite structure for A = Se or Cr). Negative values indicate the thermodynamic feasibility of the formation of mixed (ordered or disordered) Ca(CO<sub>3</sub>)<sub>1-x</sub>(AO<sub>4</sub>)<sub>x</sub> compounds. **Figure 3** shows the calculated mixing enthalpies for 0 < x < 0.25 with A being Sulfur (**left panel**), Selenium (**medium panel**) and Chromium (**right panel**). In all cases positive mixing enthalpies are obtained, regardless of the concentration (x value), nature of the tetrahedral AO<sub>4</sub> group (S, Cr or Se) and structure of the CaCO<sub>3</sub> polymorph (calcite, aragonite or vaterite). This indicates that thermodynamically a mixture of the corresponding CaCO<sub>3</sub> and CaAO<sub>4</sub> minerals is favoured over the formation of Ca(CO<sub>3</sub>)<sub>1-x</sub>(AO<sub>4</sub>)<sub>x</sub> at low temperature. A trend of increasing enthalpy values with the concentration of AO<sub>4</sub> groups (x) is observed for the three polymorphs (**Figure 3**).

For any given AO<sub>4</sub> concentration the enthalpy of mixing is lower for the vaterite polymorph than for either calcite or aragonite, independently of the crystallographic model utilized in the calculation ( $P6_3/cmm$  or *Ama2*). Enthalpies of mixing in the calcite structure are only about 1 kJ/mol higher than those of the most stable vaterite polymorph (for a more detailed scale see S.I.2). Incorporation of tetrahedral groups is by far less favourable in the aragonite polymorph, with mixing enthalpy differences respective to vaterite of the order of 4 kJ/mol. Although not shown in **figure 3**, the calculated mixing enthalpy in the aragonite phase raises to about 45 kJ/mol at x = 0.25. These results agree well with a recent DFT investigation<sup>64</sup>, where the energetic feasibility of incorporating SO<sub>4</sub> groups in CaCO<sub>3</sub> polymorphs follows the sequence vaterite > calcite >> aragonite. It should be noticed that such investigation is constricted to SO<sub>4</sub><sup>=</sup>/CO<sub>3</sub><sup>=</sup> ratios of 0.066 (calcite) 0.032 (aragonite) and 0.058 (vaterite)<sup>64</sup>. In contrast with the results of this work, our previous atomistic modelling study<sup>32</sup> found negative energies for the incorporation of sulfate groups in vaterite- $P6_3/mmc$ . However, in such investigation the mixing energies refer to the averaged  $P6_3/mmc$  structure for the three possible orientations of the carbonate groups. The present work is constricted to the most favourable orientation, which could penalize the formation of mixed Ca(CO<sub>3</sub>)<sub>1-x</sub>(SO<sub>4</sub>)<sub>x</sub>.

Regarding the nature of the AO<sub>4</sub> group incorporated (A = S, Se or Cr), at a given concentration the mixing enthalpy raises from sulfate to seleniate or chromate groups, making less thermodynamically feasible the formation of the doped Ca(CO<sub>3</sub>)<sub>1-x</sub>(AO<sub>4</sub>)<sub>x</sub> vaterites for A = Se, Cr. A strict chemical comparison of the investigated AO<sub>4</sub> groups is difficult due to the distinct A electronic configurations ( $np^4$  for calcogenides S and Se and  $d^4$  for transition metal Cr). However, one can expect the volume of the tetrahedral group to be the main factor in determining the mixing enthalpies. As a first indicative of the tetrahedral group volume, the ionic radii of A in coordination number four can be considered, being 0.12 Å for S<sup>6+</sup>, 0.26 Å for Se<sup>6+</sup> and 0.30 Å for Cr<sup>+6</sup><sup>66</sup>. Secondly, the tetrahedral group volume can be estimated from the calculated A-O distances in the Ca(CO<sub>3</sub>)<sub>1-x</sub>(AO<sub>4</sub>)<sub>x</sub>O<sub>3</sub> structures. The calculated bond lengths

fall in the ranges 1.45-1.50 Å (S-O), 1.63-1.69 Å (Se-O) and 1.62-1.69 Å (Cr-O). As seen in **figure 3** the nature of the  $\text{AO}_4$  group have a quantitative effect on the mixing enthalpies. The greater  $\text{AO}_4$  groups raise the mixing enthalpy values for all the polymorphs, being this trend more notorious at larger  $x$  values. For instance, considering incorporation of  $\text{AO}_4^{2-}$  in the calcite structure, for  $x = 0.021$  the energy mixing values (kJ/mol) are 2.4 (S), 2.7 (Se) and 2.6 (Cr) kJ/mol; this is, the larger sizes of Se and Cr penalize the incorporation of the respective  $\text{AO}_4^{2-}$  groups in about 0.3 kJ/mol. Though this small difference cannot

be considered significant enough to derive conclusions on the size-related effect of the incorporation of tetrahedral oxoanions on the energetics of  $\text{CaCO}_3$  polymorphs, this particular trend becomes more evident when higher substituting levels are considered. Thus, for  $x = 0.167$  the values are 12.5 (S), 14.9 (Se) and 16.0 (Cr) kJ/mol, with a penalty of around 3 kJ/mol for the incorporation of the larger  $\text{SeO}_4^{2-}$  and  $\text{CrO}_4^{2-}$  groups.

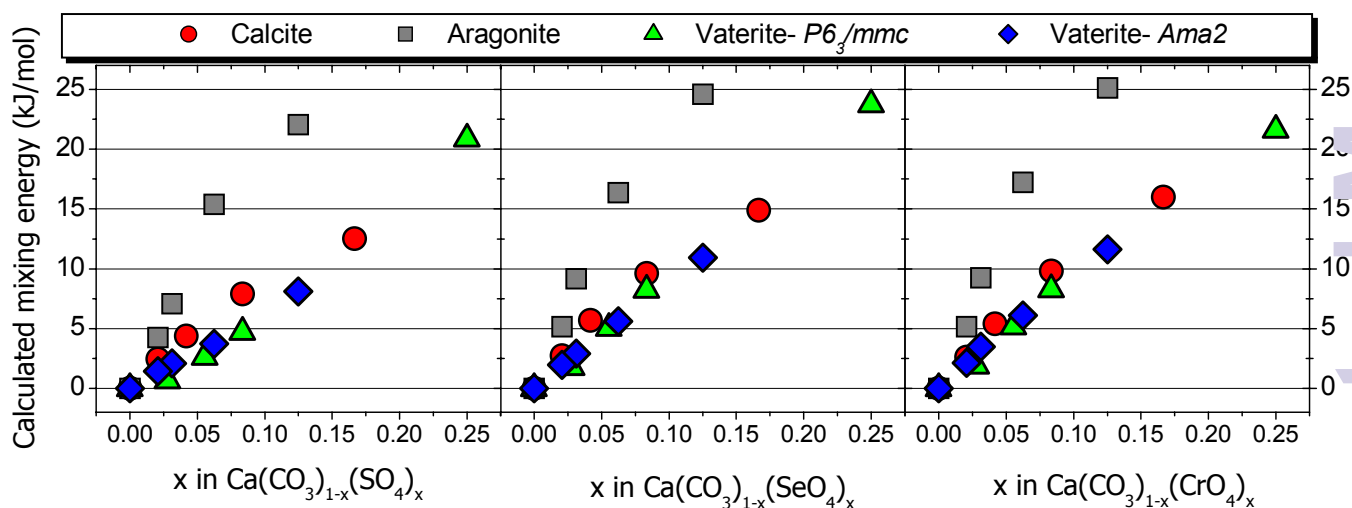


**Figure 3.-** Calculated mixing energies of  $\text{Ca}(\text{CO}_3)_{1-x}(\text{AO}_4)_x$  in the crystal structures of calcite (red circles) aragonite (grey squares) and Vaterite- $\text{P6}_3/\text{mmc}$  (green triangles) and vaterite-*Ama2* (blue diamonds). A magnification of the figure for  $x < 0.1$  is given in S.I.

Even if the reaction (1) has a positive reaction enthalpy, this reaction might still be thermodynamically feasible if it were accompanied by a large enough positive entropy of mixing. In this case, the transformation could become favourable at temperatures above 0 K ( $\Delta G_r = \Delta H_r - T\Delta S_r$ ). At low  $\text{AO}_4^{2-}$  concentrations ( $x < 0.03$ ), the mixing enthalpy for sulfate groups is much smaller than the thermal energy at room temperature ( $K_B T = 2.5$  kJ/mol), with a minimum value of 0.7 kJ/mol for vaterite- $\text{P6}_3/\text{mmc}$  making the incorporation of tetrahedral groups in vaterite quite likely. On the contrary, the larger enthalpies of mixing for the aragonite polymorph (minimum values of 5 kJ/mol) suggest that even considering entropic factors the incorporation of tetrahedral groups in this polymorph would still be precluded.

**Relative stability of doped polymorphs.** **Figure 3** suggests that a low concentration of tetrahedral groups can be incorporated in  $\text{CaCO}_3$  polymorphs at moderate temperatures, the incorporation being increasingly unfavourable in the order vaterite, calcite, aragonite. Assuming the formation of  $\text{Ca}(\text{CO}_3)_{1-x}(\text{AO}_4)_x$  phases, next we investigate the relative stability of the  $\text{Ca}(\text{CO}_3)_{1-x}(\text{AO}_4)_x$  polymorphs in the structures

of calcite, aragonite and vaterite. The corresponding reaction is written as:



**Figure 4** shows the difference in calculated total energy of aragonite and vaterite  $\text{Ca}(\text{CO}_3)_{1-x}(\text{AO}_4)_x$  relative to the calcite polymorph for A being Sulfur (**left panel**), Selenium (**medium panel**) and Chromium (**right panel**). This figure has been constructed from the data collected in **fig 2 of S.I**. Positive energy difference means an energetically less stable state. As seen in **figure 4**, the relative energetic stability is almost independent of the nature of the tetrahedral group. Calcite remains as the most stable polymorph, while the presence of tetrahedral groups greatly destabilizes the densest aragonite structure. At the reasonable doping concentrations ( $x < 0.1$ ), the relative energy of any of the two vaterite models respective to calcite is slightly decreasing. Generally speaking, for higher concentrations (not reachable in practise), the trend is that vaterite lowers its energy respective to the calcite phase.

These results indicate that, even though incorporation of tetrahedral groups is more favoured in vaterite structure, the resulting vaterite- $\text{Ca}(\text{CO}_3)_{1-x}(\text{AO}_4)_x$  would transform to the thermodynamically stable phase calcite- $\text{Ca}(\text{CO}_3)_{1-x}(\text{AO}_4)_x$ . It should be noted that at room temperature one must account for the entropy. The softer vaterite phase has a larger entropy than the calcite phase ( $S_{298}^{\circ}\text{vaterite} = 93.01 \text{ J/Kmol}$ ,  $S_{298}^{\circ}\text{calcite} =$

$91.71 \text{ J/Kmol}$ <sup>67</sup>). Similar differences can be expected between doped vaterite and calcite. This is to say, at room temperature, the entropy contribution might lower the free energy of  $\text{AO}_4$ -vaterite relative to  $\text{AO}_4$ -calcite. In the end, the effect of the incorporation of tetrahedral groups is to diminish the driving force for the vaterite to calcite transformation.

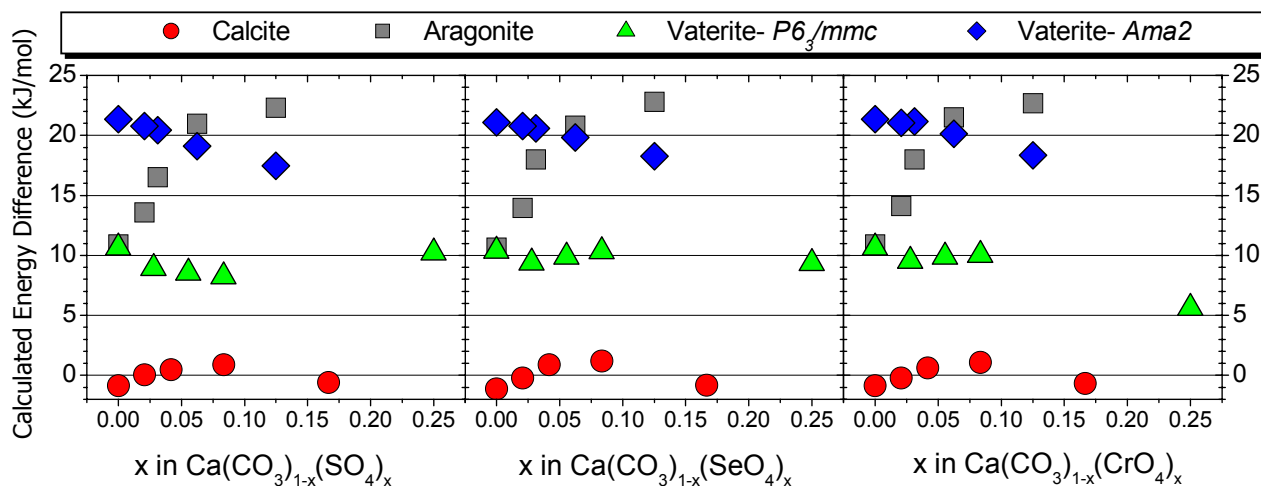


**Figure 4.-** Relative energetic stability of  $\text{Ca}(\text{CO}_3)_{1-x}(\text{AO}_4)_x$  in the crystal structures of calcite (red circles) aragonite (grey squares), vaterite-P6<sub>3</sub>/mmc (green triangles) and vaterite-Ama2 (blue diamonds). The zero of energy is taken from the linear fit of the calculated calcite total energy vs composition (see S.1.2).

## Discussion

First principles calculations indicate that the incorporation of  $\text{AO}_4^{2-}$  groups substituting  $\text{CO}_3^{2-}$  groups in the structure of  $\text{CaCO}_3$  polymorphs is energetically more feasible for vaterite, less so for calcite and very unfavourable for aragonite. The different capability of  $\text{CaCO}_3$  polymorphs to incorporate tetrahedral groups seems to be linked to their density ( $d_{\text{aragonite}} > d_{\text{calcite}} > d_{\text{vaterite}}$ ), so that the softer the polymorph the lower the enthalpy of mixing. These results are in good agreement with previous modelling studies of the substitution of  $\text{SO}_4^{2-}$  groups into  $\text{CaCO}_3$  polymorphs<sup>32, 64</sup> and are compatible with molecular dynamics calculations of the energetics of sulfate adsorption on calcite and aragonite surfaces<sup>27</sup>. These results agree well with the observed formation of a higher proportion of vaterite when  $\text{CaCO}_3$  precipitates from sulfate<sup>32</sup>, chromate<sup>24</sup> or selenate<sup>23</sup>-bearing aqueous solutions. Although our results do not predict stability crossovers resulting from  $\text{AO}_4^{2-}$  groups incorporation into  $\text{CaCO}_3$  polymorphs, they strongly support a reduction of the driving force for the transformation of  $\text{AO}_4$ -bearing vaterite into the thermodynamically stable calcite. Moreover, the stabilization of  $\text{AO}_4$ -bearing vaterite with respect to pure calcite or  $\text{AO}_4$ -bearing calcite at temperatures above 0K cannot totally be discarded. In fact, experimental observations

of  $\text{CaCO}_3$  crystallization in the presence of  $\text{CrO}_4^{2-}$  and  $\text{SeO}_4^{2-}$  seem to support such stabilization of vaterite.

Beyond the thermodynamics of  $\text{CaCO}_3$  polymorphs, kinetics issues must be discussed. The activation energy for the vaterite to calcite phase transition in the solid state is of 250 kJ/mol<sup>2, 41</sup>. In the presence of an aqueous phase this phase transition would occur through a mechanism which involves a dissolution-crystallization process, for which the activation energy is 55 kJ/mol<sup>68</sup>. This much smaller activation energy makes the dissolution-crystallization mechanism a more likely one under Earth surface conditions than the solid state transformation. The driving force for solvent mediated polymorphic transformations is the difference in solubility between the two polymorphs involved in the process<sup>69</sup>. It is well known that the solubility of solid solutions is composition dependent and relates to the solubilities of the end-members in a way that depends on the degree of ideality/non-ideality of this solid solution<sup>70-73</sup>. Consequently, the solubilities of  $\text{AO}_4$ -vaterite and  $\text{AO}_4$ -calcite will differ from those of pure vaterite and pure calcite. The change in solubility of each polymorph as a function of their  $\text{AO}_4^{2-}$  content will relate to the enthalpy change resulting from  $\text{AO}_4^{2-}$  incorporation. Since the enthalpy difference between doped-vaterite and doped-calcite decreases as their  $\text{AO}_4^{2-}$  content increases, the difference in solubility between these polymorphs will also decrease as they

incorporate higher amounts of  $\text{AO}_4^{2-}$  substituting  $\text{CO}_3^{2-}$ . The direct consequence of these changes in solubility will be a reduction of the driving force for the solvent mediated transformation of doped-vaterite into doped calcite.

The above solubility considerations play a key role in ageing experiments of  $\text{CaCO}_3$  precipitated from chromate-bearing aqueous solutions<sup>23-25</sup>. These experiments rendered a progressively more sluggish kinetic for the coupled dissolution-crystallization transformation of vaterite into calcite as the initial concentration of  $\text{CrO}_4$  in the growth medium was higher<sup>24, 74</sup>. This change in the kinetics of the transformation can be interpreted as the result of a progressive reduction of the difference in solubility between vaterite-type and calcite-type  $\text{Ca}(\text{CO}_3)_{1-x}(\text{CrO}_4)_x$  solid solution as the amount of  $\text{CrO}_4$  is higher. The direct consequence of this reduction of the difference in solubility is the decrease of the driving force for the solvent mediated polymorphic transformation between the vaterite-type and the calcite-type phases.

The influence of sulfate in the crystallization of  $\text{CaCO}_3$  has been far more studied than that of chromate and selenate. Paradoxically, rather than bringing up a clearer picture, the results of different studies seem to be contradictory. All experimental studies point to the sulfate presence in the growth medium strongly affecting  $\text{CaCO}_3$  polymorph selection. However, while according to a number of those studies sulfate favors the formation of vaterite<sup>32, 33</sup> and inhibits its transformation into calcite, there is also significant experimental evidence that sulfate stabilizes aragonite<sup>26, 28, 29</sup>. According to the results of the present work, even if vaterite does not effectively become the most stable  $\text{CaCO}_3$  polymorph at 0K conditions, the energies of vaterite and calcite containing equal amounts of sulfate are progressively closer as the concentration of sulfate increases. Since similar conclusions were previously obtained in other modelling studies<sup>32, 64</sup>, it must be concluded that, even if the formation of vaterite in the first place results from the predominance of kinetics over thermodynamics, thermodynamic factors control the stabilization of sulfate-bearing vaterite with respect to calcite in a similar way as described for chromate-bearing vaterite. Contrarily to the behavior of vaterite, the energy of aragonite rapidly increases with sulfate incorporation. Therefore, the reasons underlying the stabilization of this polymorph in the presence of sulfate cannot be thermodynamic but kinetic. In addition to the solubilities of the polymorphs a plethora of other physicochemical parameters of the solution (pH,  $\text{CO}_3^{2-}/\text{AO}_4^{2-}$  ratio, temperature, presence of other foreign ions...) can play a role promoting or hindering the development of solvent mediated transformations between  $\text{CaCO}_3$  polymorphs. A good example is provided by the nucleation of metastable aragonite in solutions with Mg:Ca ratios consistent with modern sea water<sup>65</sup>. Unravelling this role in each particular system will require to conduct specifically design experiments.

## Conclusions

*Density Functional Theory*, without the need of any experimental input, is a powerful tool to extend our previous atomistic modelling investigation on sulfate incorporation in  $\text{CaCO}_3$  polymorphs to the incorporation of other tetrahedral groups. The computational results confirm that the incorporation of  $\text{AO}_4^{2-}$  groups substituting  $\text{CO}_3^{2-}$  groups is energetically more feasible for vaterite, less so for calcite and very unfavourable for aragonite, with the larger tetrahedral groups (selenate and chromate) introducing a penalty in the mixing energies compared to that resulting from sulfate incorporation. Although at 0 K calcite remains as the most stable polymorph in all the systems for the range of  $\text{AO}_4^{2-}$  substitution considered, the calculated enthalpy difference between vaterite and calcite decreases as the concentration of incorporated tetrahedral groups increases. This result has as a consequence a decrease in the driving force for the transformation of doped vaterite into doped or pure calcite, explaining the numerous experimental observations of a progressively delayed transformation of doped-vaterite to doped-calcite during aging in contact with an aqueous solution as the concentration of  $\text{AO}_4^{2-}$  in the fluid phase is higher.

Computational results contribute to draw a clearer picture of the thermodynamics of  $\text{Ca}(\text{CO}_3)_{1-x}(\text{AO}_4)_x$  polymorphs. However, in order to interpret observations in both experimental systems and natural media, kinetic effects need also be considered. Indeed, under Earth surface and subsurface temperatures, most solid state transformations between polymorphs are kinetically hindered and routes involving dissolution-recrystallization processes dominate mineral reactions. The progress of these processes is unavoidably affected by the nature and concentration of ions present in the media ( $\text{Ca}^{2+}$ ,  $\text{Mg}^{2+}$ ,  $\text{CO}_3^{2-}$ ,  $\text{HCO}_3^-$ ,  $\text{AO}_4^{2-}$ ...). Taking into consideration all physicochemical factors that can play a role in the stabilization/transformation of  $\text{CaCO}_3$  polymorphs should help to conciliate the results of computational approaches and the diversity of experimental observations made to the date.

## Acknowledgements

This research was supported by MICINN-Spain, under grants CGL2010-20134-C02-0, CGL2010-20134-C02-02, MAT 2011-22753, and CSD2007-00045 and by the German Federal Ministry of Education and Research (ImmRad: Basic research on Immobilization of long-lived Radionuclides by interaction with relevant secondary repository-phases). M.E. Arroyo acknowledges access to computational resources from Universidad de Oviedo (MALTA cluster) and the Spanish's national high performance computer service (I2 Basque Centre).

## Notes and references

<sup>1</sup> Dpto. de Química Inorgánica, Facultad de Ciencias Químicas, Universidad Complutense de Madrid, 28040-Madrid (Spain)



<sup>2</sup> Departamento de Geología, Universidad de Oviedo, 33005 Oviedo, Spain

<sup>3</sup> Departamento de Cristalografía y Mineralogía, Universidad Complutense de Madrid, 28040 Madrid, Spain

† Corresponding author: [e.arroyo@quim.ucm.es](mailto:e.arroyo@quim.ucm.es)

## References

1. W. D. Carlson, *Rev. Mineral.*, 1983, **11**, 191-225.
2. A. V. Radha and A. Navrotsky, *Rev. Min. Geochem.*, 2013, **77**, 73-121.
3. D. Gebauer, P. N. Gunawidjaja, J. Y. P. Ko, Z. Bacsik, B. Aziz, L. Liu, L. Bergström, C.-W. Tai, T.-K. Sham, M. Eden and N. Hedin, *Angew. Chem.*, 2010, **122**, 9073-9075.
4. F. C. Meldrum and H. Cölfen, *Chem. Rev.*, 2008, **108**, 4332-4432.
5. R. Sheikholeslami and H. W. K. M. Ong, 2003, **157**, 217-234.
6. H. D. Schulz and M. Zabel *Marine Geochemistry*, 2007.
7. T. W. May, J. F. Fairchild, J. D. Petty, M. J. Walther, J. Lucero, M. Delvaux, J. Manring and M. Armbruster, *Environmental Monitoring and Assessment*, 2008, **137**, 213-232.
8. S. A. Katz and H. Salem, eds., *The biological and environmental chemistry of chromium*, VCH., New York, 1994.
9. J. O. Nriagu and E. Nieboer, *Chromium in the Natural and Human Environments*, John Wiley & Sons, New York, 1988.
10. G. Jörg, R. Bühnenmann, S. Hollas, N. Kivel, K. Kossert, S. Van Winkel and C. L. Gostomski, *Applied Radiation and Isotopes*, 2010, **68**, 2339-2351.
11. A. L. Ryser, D. G. Strawn, M. A. Marcus, S. Fakra, J. L. Johnson-Maynard and G. Möller, *Environmental Science & Technology*, 2006, **40**, 462-467.
12. G. Olyslaegers, T. Zeevaert, P. Pinedo, L. Simon, G. Prohl, R. Kowe, Q. Chen, S. Mobbs, U. Bergström, B. Hallberg, T. Katona, K. Eged and B. Kanyar, *J. Radiological Protection*, 2005, **25**, 375-392.
13. M. Prieto, J. M. Astilleros and L. Fernández-Díaz, *Elements*, 2013, **9**, 195-201.
14. S. J. Traina and V. Laperche, *Proc. Natl. Acad. Sci. USA* 1999, **99**, 3365-3371.
15. J. González-López, S. E. Ruiz-Hernández, A. Fernández-González, A. Jimenez, N. H. de Leeuw and R. Grau-Crespo, *Geochim. Cosmochim. Acta*, 2014, **142**, 205-216.
16. R. J. Reeder, G. M. Lambie, J. F. Lee and W. J. Staut, *Geochim. Cosmochim. Acta*, 1994, **58**, 5639-5646.
17. W. J. Staudt, R. J. Reeder and A. A. Schoonen, *Geochim. Cosmochim. Acta*, 1994, **58**, 2087-2089.
18. Y. Tang, E. J. Elzinga, Y. J. Lee and R. J. Reeder, *Geochim. Cosmochim. Acta*, 2007, **71**, 1480-1493.
19. Y. Kitano, M. Okumura and M. Idogaki, *Geochem. J.*, 1975, **9**, 75-84.
20. E. Busenberg and L. N. Plummer, *Geochim. Cosmochim. Acta*, 1985, **49**, 713-725.
21. R. K. Takesue, C. R. Bacon and J. K. Thompson, *Geochim. Cosmochim. Acta*, 2008, **72**, 5431-5445.
22. T. Yoshimura, A. Tamemori, R. Suzuki, N. Nakashima, H. Iwasaki, H. Hasegawa and H. Kawahata, *Chemical Geology*, 2013, **352**, 170-175.
23. A. Fernández-González and L. Fernández-Díaz, *Am. Min.*, 2013, **98**, 1824-1833.
24. B. Hua, B. L. Deng, E. C. Thorton, J. Yang and J. E. Amonette, *Water Oil and Soil Pollution*, 2007, **179**, 381-390.
25. N. Sanchez-Pastor, A. M. Gigler, J. A. Cruz, S.-H. Park, G. Jordan and L. Fernandez-Diaz, *Crystal Growth & Design*, 2011, **11**, 3081-3089.
26. P. Dydo, M. Turek and J. Ciba, *Desalinization*, 2003, 245-251.
27. Y. Tang, F. Zhang, Z. Cao, W. Jing and Y. Chen, *Journal of Colloid and Interface Science*, 2012, **377**, 430-437.
28. P. Bots, L. G. Benning, R. R.E.M. and S. Shaw, *Gelogy*, 2011, **39**, 331-334.
29. R. M. Wagtervel, M. Yu, G. J. Miedema and G. J. Witkamp, *Journal of Crystal Growth* 2014, **387**, 29-35.
30. S. E. Grasby, *Geochimica et Cosmochimica Acta*, 2003, **67**, 1659-1666.
31. F. Jroundi, M. T. González-Muñoz, A. García-Bueno and C. Rodríguez-Navarro, *Acta Biomaterialia* 2004, **10**, 3844-3854
32. L. Fernandez-Díaz, A. Fernandez-Gonzalez and M. Prieto *Geochimica Et Cosmochimica Acta*, 2010, **74**, 6064-6076.
33. L. Fernández-Díaz, C. M. Pina, J. M. Astilleros and N. Sánchez-Pastor, *Am. Mineral.*, 2009, **94**, 1223-1234.
34. S. Weiner and P. M. Dove, *Rev. Min. Geochem.*, 2003, **54**, 1-29.
35. H. E. Dunsmore, *Energy Convers. Mgmt.*, 1992, **33**, 565-572.
36. A. V. Radha, T. Z. Forbes, C. E. Killian, P. U. P. A. Gilbert and A. Navrotsky, *Proc. Natl. Acad. Sci. USA*, 2010, **107**, 16438-16443.
37. N. L. Allan, A. L. Rohl, D. H. Gay, C. C.R.A., R. J. Davey and E. C. Mackrodt, *Faraday Discuss.*, 1993, **95**, 273-280.
38. U. Becker, P. Risthaus, F. Brandt and D. Bosbach, *Chemical Geology*, 2006, **225**, 244-255.
39. A. L. Roht, K. Wright and J. D. Gale, *Am. Mineral.*, 2003, **88**, 921-925.
40. R. Demichelis, P. Raiteri, J. D. Gale and R. Dovesi, *Crystal Growth & Design*, 2013, **13**, 2247-2251.
41. J. Wang and U. Becker, *Am. Mineral.*, 2012, **97**, 1427.
42. H. J. Meyer, *Angew. Chem.*, 1959, **71**, 678-679.
43. A. Le Bail, S. Ouhenia and D. Chateigner, *Powder Diffraction*, 2011, **26**, 16-21.
44. S. R. Kamhi, *Acta Crystallographica*, 1963, **16**, 770-772.
45. J. Wang and U. Becker, *American Mineralogist*, 2009, **94**, 380-386.
46. R. Demichelis, P. Raiteri, J. D. Gale and R. Dovesi, *CrystEngComm*, 2012, **14**, 44-47.
47. J. D. C. McConnell, *Min. Mag.*, 1960, **32**, 535-544.
48. E. Mugnaioli, I. Andrusenko, T. Schüller, N. Loges, R. E. Dinnebier, M. Panthöfer, W. Tremel and U. Kolb, *Angew. Chem.*, 2012, **51**, 7041-7045.
49. G. Kresse and J. Furthmuller, *Computer Matter. Science*, 1996, **15**, 1-3.
50. G. Kresse and D. Joubert, *Phys. Rev. B*, 1999, **59**, 1758.
51. J. P. Perdew, K. Burke and M. Ernzerhof, *Physical Review Letters*, 1996, **77**, 3865-3868.
52. M. E. Arroyo-de Dompablo, P. Rozier, M. Morcrette and J. M. Tarascon, *Chem Mater*, 2007, **19**, 5411-5422.
53. M. E. Arroyo-de Dompablo, A. Morales and M. Taravillo, *J. Chem. Phys.*, 2011, **135**, 054503-054511.
54. P. E. Bloch, *Phys. Rev. B*, 1994, **50**, 17953.

55. D. L. Graf, *American Mineralogist*, 1961, **46**, 1283-1316.
56. De Villiers.J.P.R. , *American Mineralogist*, 1971, **56**, 758-772.
57. F. C. Hawthorne and R. B. Ferguson, *The Canadian Mineralogist* 1975, **13**, 289-292.
58. J. Clouse, *Zeitschrift für Kristallographie*, 1932, **83**, 161-171.
59. F. D. Murnaghan, *Proc. Natl. Acad. Sci. USA* 30, 1944, **30**, 244-247.
60. A. R. Oganov and C. W. Glass, *Journal of Chemical Physics*, 2006, **124**.
61. D. P. Dandekar and A. L. Ruoff, *J. Applied Physics*, 1986, 6004-6009.
62. S. Ono, T. Kikegawa, Y. Ohishi and J. Tsuchiya, *Am. Mineral.*, 2005, **90**, 667-671.
63. A. Jain, S. P. Ong, G. Hautier, W. Chen, W. D. Richards, S. Dacek, S. Cholia, D. Gunter, D. Skinner, G. Ceder and K. A. Persson, *Applied Physics Letters Materials*, 2013, **1(1)**, 011002.
64. E. Balan, M. Blanchard, C. Pinilla and M. Lazzeri, *Chemical Geology*, 2014, **374-375**, 84-91.
65. W. Sun, J. Saivenkataraman, W. Chen, K. A. Persson and G. Ceder, *Proc. Natl. Acad. Sci. USA*, 2015, **112** 3199-3204.
66. R. D. Shannon, *Acta Cryst.*, 1976, **A32**, 751-767.
67. K. Königsberger, L.-C. Königsberger and H. Gamsjäger, *Geochim. Cosmochim. Acta*, 1999, **63**, 3105-3119.
68. D. Kralj, L. Brečević and J. Kontrec, *Journal of Crystal Growth*, 1997, **177**, 248-257.
69. P. T. Cardew and R. J. Davey, *Proc. R. Soc. London*, 1985, **A 398**, 415-428.
70. J. M. Astilleros, C. M. Pina, Fernández-Díaz and A. L. Putnis, *Surface Science*, 2003, **545**, 767-773.
71. P. D. Glynn, *Rev. Min.* , 2000, **40**, 481-511.
72. M. Prieto, *Reviews in Mineralogy & Geochemistry*, 2009, **70**, 47-85.
73. M. Prieto, J. M. Astilleros, C. M. Pina, L. Fernández-Díaz and A. Putnis, *Am. J. Sci.*, 2007, **307**, 1034-1045.
74. J. Cruz, N. Sánchez-Pastor, A. M. Gigler and L. Fernández-Díaz, *Spectroscopy Letters*, 2011, **44**, 495-499.